

Wideband DOA Estimation Algorithms for Multiple Target Detection and Tracking Using Unattended Acoustic Sensors

Mahmood R. Azimi-Sadjadi^{*a}, Ali Pezeshki^b, Louis L. Scharf^{b †} and Myron Hohil^c

^aInformation System Technologies, Inc, Fort Collins, CO 80521

^bColorado State University, Fort Collins, CO 80523

^c US Army TACOM-ARDEC, Picatinny Arsenal, NJ 07806

ABSTRACT

The problem of detection, tracking and localization of multiple wideband sources (ground vehicles) using unattended passive acoustic sensors is considered in this paper. Existing methods typically fail to detect, resolve and track multiple closely spaced sources in tight formations, especially in the presence of clutter and wind noise. In this paper, several existing wideband direction of arrival (DOA) estimation algorithms are extended and applied to this problem. A modified version of the Steered Covariance Matrix (STCM) algorithm is presented that uses a two-step search process. To overcome the problems of existing DOA estimation methods, new wideband versions of the narrowband Capon beamforming method are proposed that use various algorithms for combining power spectra from different frequency bins. These methods are then implemented and benchmarked on a real acoustic signature data set that contains multiple ground targets moving in tight formations.

Keywords: DOA estimation, sparse sensor arrays, steered covariance matrix, Capon beamforming.

1. INTRODUCTION

The problem of detection, classification and localization of multiple ground targets, e.g. trucks and tanks, using unattended passive acoustic sensors is complicated due to various factors. These include: variability and nonstationarity of target acoustic signatures, signal attenuation and fading effects as a function of range and doppler, extremely low signal-to-noise ratio (SNR) in certain terrain and environmental conditions, competing interference sources forming signatures with similar characteristics as those of the actual targets, obscured targets, and lack of a priori information about the target initial conditions. In addition, the presence of multiple targets that are spatially close together in tight formations, e.g. staggered, abreast or single-file, further complicates the direction of arrival (DOA) estimation, detection, data association and localization processes.

The work at the Army Research Laboratory (ARL)¹⁻³ involves development of array signal processing algorithms using small baseline acoustic arrays to track and classify moving targets from their acoustic signatures. Since conventional beamforming schemes generally do not provide good results in these situations, owing to the structural limitations of the array and lack of spatial coherence, data dependent high-resolution DOA algorithms must be developed. Current efforts on incoherent and coherent wideband MUSIC⁴ (Multiple Signal Classification) show some promise for detecting and tracking multiple ground vehicles. In ref,² by exploiting the multi-spectral content of the targets, better results were reported using wideband signal subspace DOA algorithms. Experimental results using a circular array of six sensors, with a diameter of 8 ft indicated the advantages of the wideband MUSIC over the delay-sum algorithm. In ref³ focused wideband adaptive array processing algorithms are employed for the high-resolution DOA estimation of ground vehicles. Several methods including Steered Covariance Matrix (STCM)⁵⁻⁶ and spatial smoothing or interpolation⁵ using the array manifold interpolation are considered. In addition, this study provides experimental analysis of incoherent and coherent wideband MUSIC algorithms and narrowband MUSIC for a circular array of acoustic sensors in terms of accuracy of DOA estimates. It is shown that for certain SNR conditions incoherent wideband methods yield more accurate DOA estimates than the coherent methods for highly peaked spectra while for sources with flat spectra the coherent wideband methods generate more accurate DOA estimates. The study indicates that the

fno@infsyst.biz; phone: 1 970 224 2556; fax 1 970 224 2556

†. Scharf and A. Pezeshki are consultants at Information System Technologies, Inc.

coherent wideband methods are much more statistically stable than the incoherent ones. The price paid for this improved stability is high computational cost.

As far as we know, none of the existing algorithms demonstrated proven capability to detect and track multiple closely spaced sources in tight formations especially in presence of high level of clutter and wind noise. This is critical in realistic battlefield scenarios where a large number of targets may be encountered under difficult environmental and terrain conditions. Recently, as part of the SBIR-Army Phase II project, Information System Technologies, Inc. (ISTI) has carried⁷ out a comprehensive study of different wideband DOA estimation algorithms and their applicability to the problem in hand. Among the methods carefully studied are the STCM⁶ and the weighted subspace fitting (WSF),^{4,8} algorithms. The original version of STCM uses a diagonal focusing matrix which can only resolve a group of closely spaced sources when all the DOA's are within one beamwidth of the focusing angle. The other choices of the focusing matrix⁹ were also found to be incapable of providing accurate and unbiased estimates of multiple closely spaced DOA's. As far as WSF method is concerned, it requires a computationally demanding multi-dimensional search to find the DOA's. Additionally, the accuracy of DOA estimation in this method is highly dependent on the choice of the initial conditions for the search process. Clearly, this limits the usefulness of the WSF method for real applications, where the sources are closely spaced and move in tight formations.

In light of all these problems, ISTI developed⁷ three new wideband DOA estimation algorithms to resolve the issues with the focusing process in the STCM algorithm and also to improve the accuracy and robustness of DOA estimation. These algorithms are based upon wideband extensions of Capon beamforming. Three different methods for combining individual power spectra at different frequency bins were also introduced. These are based upon arithmetic mean, geometric mean, and harmonic mean operations. The resultant wideband Capon beamformers possess different beam-patterns and bearing responses at various frequencies that are studied in this paper. These wideband methods were then benchmarked with the modified versions of STCM algorithm and the results on real acoustic signature data set are presented. The test results on several calibrated acoustic signature data sets that contain multiple groups of light or heavy, wheeled or tracked vehicles demonstrated that among all the methods developed or studied, geometric mean and harmonic mean wideband Capon methods provide better experimental results, in terms of accuracy of DOA estimation and their capability in resolving the individual targets within the groups, on the certain data set under study.

2. WIDEBAND DOA ESTIMATION METHODS

Let us consider an array of M sensors that receive the wavefield generated by d wideband sources in the presence of an arbitrary noise wavefield. The array geometry can be arbitrary but known to the processor. The source signal vector $\mathbf{s}(t) = [s_1(t), s_2(t), \dots, s_d(t)]^T$ is assumed to be zero mean and stationary over the observation interval T_0 . The source spectral density matrix is denoted by $P_s(f)$, $|f| \in F = [f_c - BW/2, f_c + BW/2]$ with the bandwidth BW comparable to center frequency f_c . The spectral density matrix $P_s(f)$ is a $d \times d$ nonnegative Hermitian matrix, unknown to the processor. The noise wavefield is assumed to be independent of the source signals with $M \times M$ noise spectral density matrix $P_n(f)$. Then, the spectral density matrix of the M -dimensional array output $\mathbf{x}(t)$ may be written as

$$P_{\mathbf{x}}(f) = A(f, \theta)P_s(f)A^H(f, \theta) + P_n(f) \quad (1)$$

where $A(f, \theta) = [\mathbf{a}(f, \theta_1), \mathbf{a}(f, \theta_2), \dots, \mathbf{a}(f, \theta_d)]$ is the $M \times d$ array manifold matrix of the sensor array system, with respect to some chosen reference point, $\mathbf{a}(f, \theta_i)$ is the direction vector of the i th source, and $\theta = [\theta_1, \dots, \theta_d]$ is the bearing angle vector of the sources. It is assumed that $M > d$ and that the rank of $A(f, \theta)$ is equal to d for any frequency and angle of arrival.

The array output vector $\mathbf{x}(t)$ is first decomposed into narrowband components by using a DFT over non-overlapping time segments of length ΔT . That is, the array output $\mathbf{x}(t)$, observed over T_0 seconds, is sectioned into K windows of duration ΔT seconds each. Thus, ΔT is the duration of one snapshot in the usual terminology of narrowband array processing and K is the total number of snapshots. We denote the j th narrowband

component of all the outputs obtained from the k th snapshot by the vector $\mathbf{x}_k(f_j)$, $k = 1, 2, \dots, K$, and $j = 1, 2, \dots, J$. It is also assumed that the decomposed narrowband components are independent. The goal is to determine the number of sources d and estimate the angles θ_i , $i = 1, 2, \dots, d$ from the data $\mathbf{x}_k(f_j)$, $k = 1, 2, \dots, K$; $j = 1, 2, \dots, J$. The spatial covariance matrix for the j th narrowband component $\mathbf{x}_k(f_j)$ is

$$\mathbf{R}_{\mathbf{xx}}(f_j) \approx \mathbf{P}_x(f_j) = \mathbf{A}(f_j, \theta) \mathbf{P}_s(f_j) \mathbf{A}^H(f_j, \theta) + \mathbf{P}_n(f_j), \quad j = 1, 2, \dots, J. \quad (2)$$

where ΔT is assumed to be $\Delta T = 1$. In the sequel, we present several methods for estimating the angles θ_i 's, namely modified STCM and three wideband Capon algorithms.

2.1. STCM Algorithm⁹

The idea in the STCM method is to combine the signal subspaces at different frequencies in a manner to generate a single signal subspace with algebraic properties indicative of the number of sources and angles of arrival. The idea is to find the transformation matrices $\mathbf{T}(f_j, \theta)$, $j = 1, 2, \dots, J$, referred to as ‘‘focusing matrices’’ that transfer all the narrowband frequency components $\mathbf{x}_k(f_j)$, $j = 1, 2, \dots, J$, into a single reference frequency f_0 . After all the narrowband components are focused at frequency f_0 , the wideband DOA estimation problem reduces to a narrowband problem. Thus, any of the narrowband methods (e.g. subspace-based methods) may be used to estimate the DOA's and number of targets. The focusing process has another benefit. The beamwidth of the array at narrowband frequency f_j is varying inversely with the frequency. Thus, in order to generate a coherent integration of all the frequencies in the wideband signal, a focusing is needed.

Now assume that nonsingular $M \times M$ focusing matrices $\mathbf{T}(f_j, \theta)$, $j = 1, 2, \dots, J$, exist such that

$$\mathbf{T}(f_j, \theta) \mathbf{A}(f_j, \theta) = \mathbf{A}(f_0, \theta), \quad j = 1, 2, \dots, J. \quad (3)$$

The focused array output at the k th time interval is defined as

$$\mathbf{y}_k(f_j) = \mathbf{T}(f_j, \theta) \mathbf{x}_k(f_j) \quad (4)$$

with the spatial covariance matrix

$$\mathbf{R}_{\mathbf{yy}}(f_j) = \mathbf{T}(f_j, \theta) \mathbf{R}_{\mathbf{xx}}(f_j) \mathbf{T}^H(f_j, \theta) = \mathbf{A}(f_0, \theta) \mathbf{P}_s(f_j) \mathbf{A}^H(f_0, \theta) + \mathbf{T}(f_j, \theta) \mathbf{P}_n(f_j) \mathbf{T}^H(f_j, \theta) \quad (5)$$

The focused output $\mathbf{y}_k(f_j)$ is a narrowband component at frequency f_0 . The index f_j in $\mathbf{y}_k(f_j)$ only indicates that the focused output has been obtained from the narrowband component $\mathbf{x}_k(f_j)$. The steered or focused covariance matrix \mathbf{R} may then be defined as

$$\mathbf{R}(\theta) = \sum_{j=1}^J \mathbf{R}_{\mathbf{yy}}(f_j) = \sum_{j=1}^J \mathbf{T}(f_j, \theta) \mathbf{R}_{\mathbf{xx}}(f_j) \mathbf{T}^H(f_j, \theta) \quad (6)$$

Using (3), we may rewrite $\mathbf{R}(\theta)$ as

$$\mathbf{R}(\theta) = \sum_{j=1}^J \mathbf{A}(f_0, \theta) \mathbf{P}_s(f_j) \mathbf{A}^H(f_0, \theta) + \mathbf{R}_n \quad (7)$$

where $\mathbf{R}_n := \sum_{j=1}^J \mathbf{T}(f_j, \theta) \mathbf{P}_n(f_j) \mathbf{T}^H(f_j, \theta)$.

Summary of the Modified STCM Algorithm

The steps in the modified version of the STCM method for wideband DOA estimation may be summarized as follows.

1. DFT the time windowed array output to form $\mathbf{x}_k(f_j)$, $k = 1, \dots, K$ and $j = 1, \dots, J$;

2. Form the spatial covariance matrix for each frequency component f_j using $\mathbf{R}_{\mathbf{xx}}(f_j) = \frac{1}{K} \sum_{k=1}^K \mathbf{x}_k(f_j) \mathbf{x}_k^H(f_j)$, i.e. computed over all snapshots;
3. For every bearing angle, form $\mathbf{T}(f_j, \theta)$ and then compute the steered covariance matrix $\mathbf{R}(\theta)$ using (6);
4. Find the initial estimate of the DOA, θ^* , by applying the Capon Beamformer⁴ to the steered covariance matrix,

$$P_{CAPON}(\theta) = \frac{1}{\mathbf{a}(f_0, \theta)^H \mathbf{R}^{-1}(\theta) \mathbf{a}(f_0, \theta)}$$

5. Recompute the steered covariance matrix at the location of the peaks, i.e. $\mathbf{R}(\theta^*)$;
6. Apply singular value decomposition (SVD) to the new steered covariance matrix

$$\mathbf{R}(\theta^*) = [\mathbf{U}_s \quad \mathbf{U}_n] \begin{bmatrix} \Sigma_s & \mathbf{0} \\ \mathbf{0} & \Sigma_n \end{bmatrix} \begin{bmatrix} \mathbf{U}_s^H \\ \mathbf{U}_n^H \end{bmatrix} \quad (8)$$

where $\Sigma_s = \text{Diag}(\sigma_1, \dots, \sigma_d)$, $\Sigma_n = \text{Diag}(\sigma_{d+1}, \dots, \sigma_M)$ with $\sigma_1 > \sigma_2 > \dots > \sigma_M$ and $\sigma_{d+1} = \sigma_{d+2} = \dots = \sigma_M$, \mathbf{U}_s and \mathbf{U}_n are the coherent signal and noise subspaces, respectively;

7. Find the refined DOA estimates using MUSIC algorithm⁴ by finding the peaks of

$$P_{MUSIC}(\theta) = \frac{1}{\mathbf{a}(f_0, \theta)^H \mathbf{U}_n \mathbf{U}_n^H \mathbf{a}(f_0, \theta)}$$

The choice of the focusing matrix $\mathbf{T}(f_j, \theta)$ has a major impact on the performance of the STCM method. It was shown in ref⁹ that a good focusing matrix that makes the coherent signal subspace independent of the noise power spectrum $\mathbf{P}_n(f_j)$, $j = 1, \dots, J$ is a unitary matrix i.e. $\mathbf{T}(f_j, \theta) \mathbf{T}^H(f_j, \theta) = \mathbf{I}$, $j = 1, 2, \dots, J$. We note that the focusing matrix $\mathbf{T}(f_j, \theta)$, $j = 1, 2, \dots, J$, must also satisfy the focusing equation (3). Therefore, to determine $\mathbf{T}(f_j, \theta)$'s, the following problem must be solved at all frequency bins f_j , $j = 1, \dots, J$;

$$\mathbf{T}(f_j, \theta) \mathbf{A}(f_j, \theta) = \mathbf{A}(f_0, \theta), \quad j = 1, 2, \dots, J, \quad (9)$$

subject to

$$\mathbf{T}(f_j, \theta) \mathbf{T}^H(f_j, \theta) = \mathbf{I}. \quad (10)$$

A simple unitary focusing matrix that can be used to detect the DOA of a group of closely spaced targets that move together in a tight formation is the diagonal one of the form

$$\mathbf{T}(f_j, \theta) = \text{Diag}[a_1(f_0, \theta)/a_1(f_j, \theta), a_2(f_0, \theta)/a_2(f_j, \theta) \cdots a_M(f_0, \theta)/a_M(f_j, \theta)] \quad (11)$$

where $a_i(f_j, \theta)$ is the i th element of the steering vector $\mathbf{a}(f_j, \theta)$ at the frequency f_j and bearing angle θ . Clearly, this focusing matrix is unitary. However, it can only detect one target or one group of targets and may not be used to resolve target tracks within a group.

2.2. WSF Algorithm

In this section, we present the framework for subspace fitting⁴ methods namely WSF. Consider the SVD of $\mathbf{R}_{\mathbf{xx}}$ as

$$\mathbf{R}_{\mathbf{xx}}(f_j) = [\mathbf{E}_s(f_j) \quad \mathbf{E}_n(f_j)] \begin{bmatrix} \Lambda_s(f_j) & \mathbf{0} \\ \mathbf{0} & \Lambda_n(f_j) \end{bmatrix} \begin{bmatrix} \mathbf{E}_s^H(f_j) \\ \mathbf{E}_n^H(f_j) \end{bmatrix} \quad (12)$$

where $\Lambda_s(f_j) = \text{Diag}([\lambda_1, \dots, \lambda_d])$, $\Lambda_n(f_j) = \text{Diag}[\lambda_{d+1}, \dots, \lambda_M]$, with $\lambda_1 > \lambda_2 > \dots > \lambda_{d+1}$ and $\lambda_{d+1} = \lambda_{d+2} = \dots = \lambda_M$, and $\mathbf{E}_s(f_j) \in C^{M \times d}$ and $\mathbf{E}_n(f_j) \in C^{M \times (M-d)}$ are the signal and noise subspaces, respectively. In the case where the number of sources, d , is known, $\mathbf{R}_{\mathbf{xx}}(f_j)$ can be written as

$$\mathbf{R}_{\mathbf{xx}}(f_j) = \mathbf{X}(f_j) \mathbf{X}^H(f_j) \approx \mathbf{E}_s(f_j) \Lambda_s(f_j) \mathbf{E}_s(f_j)^H \quad (13)$$

where $\mathbf{X}(f_j) = [\mathbf{x}_1(f_j), \dots, \mathbf{x}_K(f_j)]$. This implies that the data matrix, $\mathbf{X}(f_j)$, can be represented by $\mathbf{X}(f_j) = \mathbf{E}_s(f_j)\Lambda_s(f_j)^{1/2}$. More generally, we can use any other weighting matrix like $\mathbf{W}(f_j)$ which results in $\mathbf{X}(f_j) = \mathbf{E}_s(f_j)\mathbf{W}(f_j)^{1/2}$. In the most commonly used WSF method,⁴ the weighting matrix is chosen as

$$\mathbf{W}(f_j) = (\Lambda_s(f_j) - \sigma_n^2 \mathbf{I})\Lambda_s^{-1/2}(f_j). \quad (14)$$

Assuming stationarity of the observations over the snapshots, the mean-squares error (MSE) associated with the j th narrowband component over the K snapshots would be

$$\begin{aligned} E_{WSF}(f_j) &= \sum_{k=1}^K \|\mathbf{e}_k(f_j)\|^2 \\ &= \text{tr}\{\mathbf{P}_A^\perp(f_j, \theta)\mathbf{R}_{\mathbf{xx}}(f_j)\mathbf{P}_A^\perp(f_j, \theta)\} \end{aligned} \quad (15)$$

where

$$\mathbf{P}_A^\perp(f_j, \theta) = \mathbf{I} - \mathbf{P}_A(f_j, \theta) = \mathbf{I} - \mathbf{A}(f_j, \theta)\mathbf{A}^\dagger(f_j, \theta) \quad (16)$$

is the orthogonal projection complement operator onto the subspace spanned by the columns of the array response matrix $\mathbf{A}(f_j, \theta)$. For any choice of $\mathbf{W}(f_j)$ the error in (15) becomes

$$E_{WSF}(f_j) = \text{tr}\{\mathbf{P}_A^\perp(f_j, \theta)\mathbf{E}_s(f_j)\mathbf{W}(f_j)\mathbf{W}^H(f_j)\mathbf{E}_s(f_j)^H\mathbf{P}_A^\perp(f_j, \theta)\} \quad (17)$$

Note that for no noise case, $\mathbf{W}(f_j) = \Lambda_s^{1/2}(f_j)$ and the term $\mathbf{E}_s(f_j)\mathbf{W}(f_j)\mathbf{W}^H(f_j)\mathbf{E}_s(f_j)^H$ may be replaced by $\mathbf{R}_{\mathbf{xx}}(f_j)$ in which case WSF reduces to SF.

In wideband WSF, the search process for finding θ becomes

$$\theta = \arg \min_{\theta} \text{tr}\left\{\sum_{j=1}^J \mathbf{P}_A^\perp(f_j, \theta)\mathbf{E}_s(f_j)\mathbf{W}(f_j)\mathbf{W}^H(f_j)\mathbf{E}_s(f_j)^H\mathbf{P}_A^\perp(f_j, \theta)\right\} \quad (18)$$

For the unitary diagonal focusing matrix $\mathbf{T}(f_j, \theta)$ the focused version of (18) is

$$\theta = \arg \min_{\theta} \text{tr}\left\{\mathbf{P}_A^\perp(f_0, \theta)\sum_{j=1}^J [\mathbf{T}(f_j, \theta)\mathbf{E}_s(f_j)\mathbf{W}(f_j)\mathbf{W}^H(f_j)\mathbf{E}_s(f_j)^H\mathbf{T}^H(f_j, \theta)]\mathbf{P}_A^\perp(f_0, \theta)\right\} \quad (19)$$

2.3. New Wideband Capon DOA Estimation Methods

The Capon beamformer $\mathbf{C}(f_j, \theta)$ is defined as the matrix that maximizes the power at the output of the beamformer, i.e.

$$\begin{aligned} \text{tr}\{\mathbf{Q}(f_j, \theta)\} &= \text{tr}\left\{\sum_{k=1}^K \mathbf{C}^H(f_j, \theta)\mathbf{x}_k(f_j)\mathbf{x}_k^H(f_j)\mathbf{C}(f_j, \theta)\right\} \\ &= \text{tr}\{\mathbf{C}^H(f_j, \theta)\mathbf{R}_{\mathbf{xx}}(f_j)\mathbf{C}(f_j, \theta)\} \end{aligned} \quad (20)$$

under the constraint that

$$\mathbf{C}^H(f_j, \theta)\mathbf{A}(f_j, \theta) = \mathbf{I} \quad (21)$$

The problem of finding the DOA's at frequency f_j may then be formulated⁴ as

$$\min_{\theta} \text{tr}\{\mathbf{Q}(f_j, \theta)\} = \text{tr}\{[\mathbf{A}^H(f_j, \theta)\mathbf{R}_{\mathbf{xx}}^{-1}\mathbf{A}(f_j, \theta)]^{-1}\} \quad (22)$$

This minimization problem may be solved by finding the locations of the peaks of

$$q(f_j, \theta) = \frac{1}{\mathbf{a}^H(f_j, \theta)\mathbf{R}_{\mathbf{xx}}^{-1}(f_j)\mathbf{a}(f_j, \theta)} \quad (23)$$

where $\mathbf{a}(f_j, \theta)$ is one of the columns of $\mathbf{A}(f_j, \theta)$. The value of $q(f_j, \theta)$ is the power at the output of the narrowband rank-1 Capon beamformer $\mathbf{c}(f_j, \theta)$, where

$$\mathbf{c}(f_j, \theta) = \frac{\mathbf{R}_{\mathbf{xx}}^{-1}(f_j)\mathbf{a}(f_j, \theta)}{\mathbf{a}^H(f_j, \theta)\mathbf{R}_{\mathbf{xx}}^{-1}(f_j)\mathbf{a}(f_j, \theta)} \quad (24)$$

For the wideband case, where all frequency components should be taken into account, the power at the output of the narrowband Capon beamformers, i.e. $q(f_j, \theta)$, may be averaged for all narrowband frequencies f_j , $j = 1, \dots, J$. The locations of the peaks of the average output power determine the DOA estimates. Based on the averaging method used, several interesting wideband Capon DOA estimation algorithms may be developed. These are given below.

A. Arithmetic Averaging

In this case, the average output power after beamforming is obtained using the arithmetic averaging of the output powers of the narrowband Capon beamformers, i.e. $q(f_j, \theta)$. Thus, the average output power $Q_A(\theta)$ is

$$Q_A(\theta) = \sum_{j=1}^J q(f_j, \theta) = \sum_{j=1}^J \frac{1}{\mathbf{a}^H(f_j, \theta) \mathbf{R}_{\mathbf{xx}}^{-1}(f_j) \mathbf{a}(f_j, \theta)} \quad (25)$$

B. Geometric Averaging

Alternatively, the average output power after beamforming may be obtained using the geometric averaging of the output powers of the narrowband Capon beamformers, i.e. $q(f_j, \theta)$. That is, the average output power $Q_G(\theta)$ is

$$Q_G(\theta) = \prod_{j=1}^J q(f_j, \theta) = \prod_{j=1}^J \frac{1}{\mathbf{a}^H(f_j, \theta) \mathbf{R}_{\mathbf{xx}}^{-1}(f_j) \mathbf{a}(f_j, \theta)} \quad (26)$$

C. Harmonic Averaging

Finally, the average output power after beamforming may be obtained from the harmonic averaging of the output powers of the narrowband Capon beamformers, i.e. $q(f_j, \theta)$. Thus the average output power $Q_H(\theta)$ is

$$Q_H(\theta) = \frac{1}{\sum_{j=1}^J \frac{1}{q(f_j, \theta)}} = \frac{1}{\sum_{j=1}^J \mathbf{a}^H(f_j, \theta) \mathbf{R}_{\mathbf{xx}}^{-1}(f_j) \mathbf{a}(f_j, \theta)} \quad (27)$$

The DOAs' may be estimated by finding the locations of the peaks of $Q_A(\theta)$, or $Q_G(\theta)$, or $Q_H(\theta)$.

3. ANALYSIS OF WIDEBAND CAPON AND STCM ALGORITHMS

Next, we study the 2D output power of the three wideband Capon DOA and the STCM DOA estimation algorithms with respect to the true angle and the look angle. If we denote the look angle by θ and the true angle of a single source by ϕ , the steering vector for the 5-element wagon-wheel array is $\mathbf{a}(f_j, \theta) = [e^{-jk \cos \theta} \ e^{-jk \sin \theta} \ 1 \ e^{jk \cos \theta} \ e^{jk \sin \theta}]^T$ where $k = 2\pi f_j r/c$ and f_j is the j^{th} narrowband frequency, r is the radius of the array (in this case .6096 m), and c is the speed of sound in air (335 m/s). We can define a similar vector for the received signals for a narrowband source of frequency f_j as,

$$\mathbf{x}(f_j) = [e^{-jk \cos \phi} \ e^{-jk \sin \phi} \ 1 \ e^{jk \cos \phi} \ e^{jk \sin \phi}]^T \quad (28)$$

where ϕ is the actual angle. For the noise-free case, the covariance matrix of the received signal is $\mathbf{R}_{\mathbf{xx}} = \mathbf{xx}^H$. Diagonal loading of the covariance matrix was used to avoid singularity problems and to simulate noise effects.

To generate the synthesized data for this study, a set of narrowband frequencies with 16 Hz separation and equal power were used in the frequency range of 50 to 250 Hz. The reason for not considering frequencies higher than 250Hz is that the aliasing frequency for the wagon-wheel array is approximately 277Hz.⁷ Figures 1(a)-(d) show the 2D output power for the arithmetic mean, geometric mean, harmonic mean Capon, and STCM methods, respectively. These correspond to the plots of Q_A (arithmetic), Q_G (geometric), Q_H (harmonic), and P_{CAPON} (one-step STCM) with respect to true angle θ and look angle ϕ . It can easily be seen that the width of the main lobe of the geometric mean is much narrower than those of the other methods and has no noticeable side-lobe structure. The other two methods, on the other hand, do exhibit small side-lobe structures. Since the geometric mean is based upon the product operation, the lower frequencies eliminate any side-lobes, while the

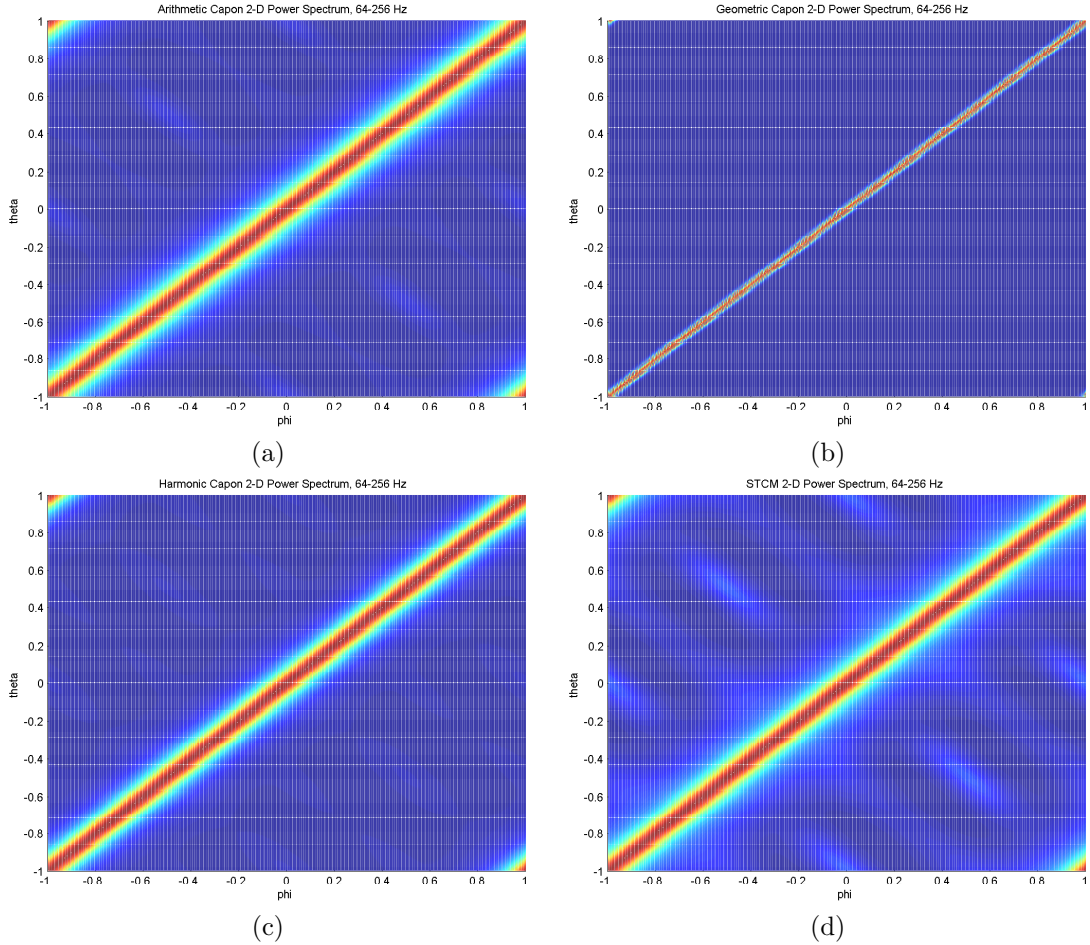


Figure 1. Power spectrums for (a) Arithmetic mean Capon, (b) Geometric mean Capon, (c) Harmonic mean Capon, and (d) STCM with respect to look direction and angle of arrival

higher frequencies narrow the beamwidth and hence giving better resolution. This may also eliminate any low-power sources located further away, as it is very difficult to distinguish between side-lobes and far away targets. Using the arithmetic and harmonic mean Capon methods some small side-lobes are inevitable and further the resolution does not improve greatly with additional frequencies. The STCM results are very similar to those of the arithmetic mean Capon, in terms of main lobe beamwidth and side-lobe structure.

4. DOA ESTIMATION RESULTS

In this section, the wideband DOA estimation algorithms described in this paper are applied to the calibrated data of two multiple target runs in the acoustic signature data set. Only the results of node 1 array are presented here owing to page limitations.

To account for the errors caused by differences between the nominal values of array parameters, namely gain, phase, and sensor positions, and the values of these parameters after the array is deployed, the data was calibrated prior to DOA estimation. The time series recorded by each microphone is first filtered using a sliding Hamming window of size 2048 (corresponding to 2 seconds of data) with 50% overlap. The calibration is then performed on each 2048 samples for the frequency range of 50-250Hz. Since the sampling frequency for the collected data set is 1024Hz and the size of the sliding Hamming window is 2048, the resultant calibrated data

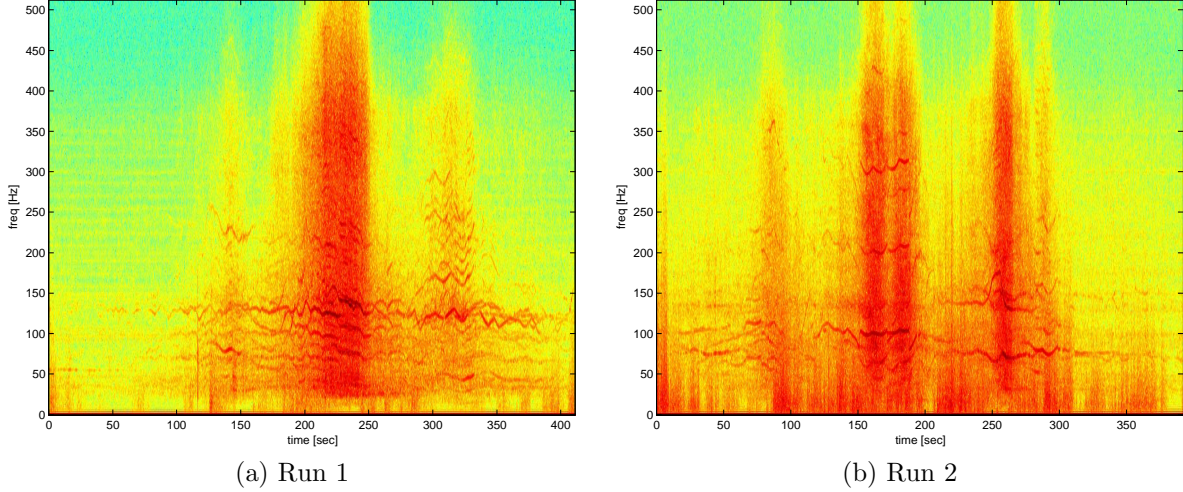


Figure 2. Spectrograms of Center Microphone of Node 1 for Runs 1 & 2

has twice the length of the uncalibrated data. Therefore, in the DOA estimation, a time window of size 2048 samples will be considered as one snapshot. In order to report a DOA estimate every second, a 50% overlap is considered between the time windows.

4.1. Results on Run 1

This run contains six targets that move in three separate groups. The first group contains a single light wheeled vehicle, the second group is formed of three heavy tracked vehicles, and the third group includes two heavy wheeled vehicles. The spectrogram of the data collected by the center microphone of node 1 for this run is shown in Figure 2(a).

Figures 3(a)-(d) show the DOA estimation results for this run, obtained using the arithmetic Capon, geometric Capon, harmonic Capon, and STCM algorithms, respectively. The actual (true) tracks are plotted in solid lines. Comparing the algorithms, clearly the geometric and the harmonic Capon provide the best results on the data set under study. This observation is also consistent with the other runs that we have considered in this study. The arithmetic mean Capon provided acceptable results, but the DOA estimates of this algorithm are not as good as those of the geometric and harmonic mean Capons. The STCM algorithm, however, performed poorly on the calibrated data as it produces several false tracks that follow certain trend, and hence may be mistaken as actual tracks. This may be explained by referring to the bearing response images for the STCM algorithms at frequency range of 50 to 250Hz. Although the upper range in the frequency band of interest is below the aliasing frequency of the array, the amplitude of the side-lobes in the bearing responses associated with the STCM algorithm are very large and comparable with the amplitude of the main-lobe. Therefore, in the peak finding procedure on the bearing response, many false peaks may be selected.

As can be seen from the results of the geometric and harmonic mean Capons for node 1 (Figures 3(b) and 3(c)) the algorithms successfully detect and track all the target groups, even the single one at far range. Moreover, these two algorithms are able to resolve the tracks of the heavy tracked vehicles, moving in a group of three in the middle, and the tracks of the two heavy wheeled vehicles, moving in a group of two on the right hand side.

The WSF algorithm was also tested on the same calibrated data set. The STCM generated estimates were used as initial estimates to define the center of a search window, with width of 61 degrees. The maximum number of sources searched for this multi-dimensional search is 2. The test results on this run indicated that compared to the results of the geometric and harmonic mean Capon methods, the WSF method provided substantially worse results. Additionally, it was observed that array calibration did not make a major difference in the results of the WSF method. Consequently, these results are not presented in this section.

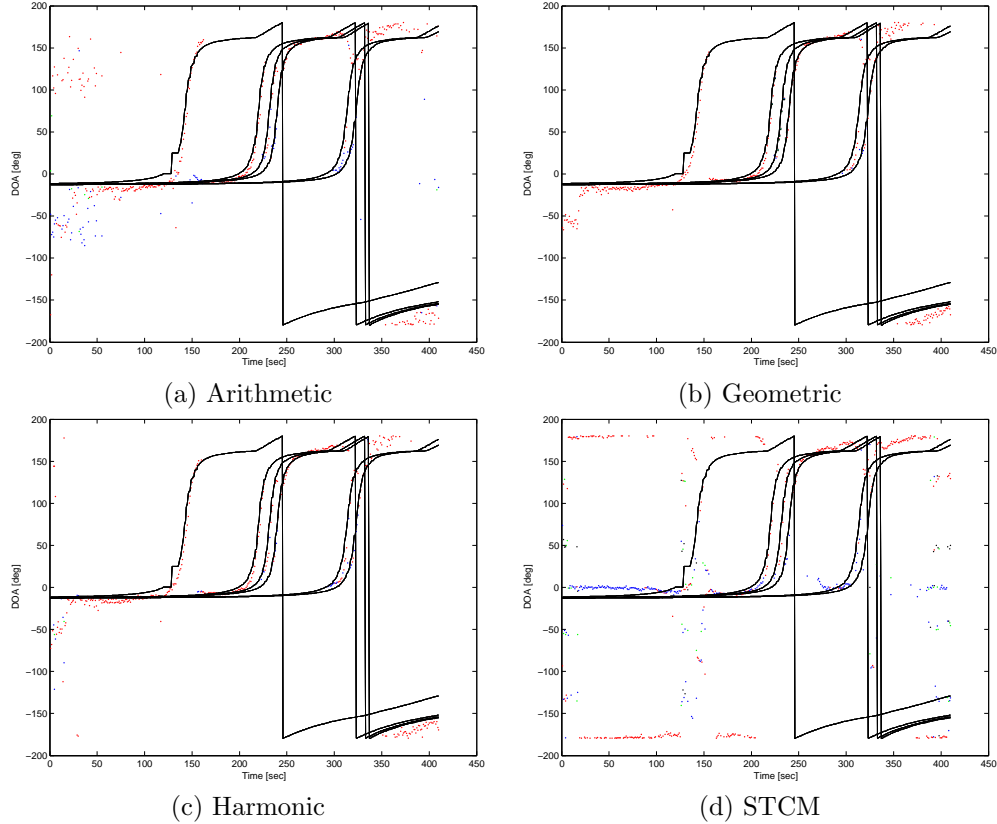


Figure 3. DOA Estimates for Run 1, obtained using Arithmetic, Geometric, Harmonic Mean Wideband Capon, and STCM Algorithms.

4.2. Results on Run 2

This run contains four moving and two stationary targets. These are: four light wheeled, and two light tracked vehicles. Unfortunately, we do not have the information as to which track corresponds to which target. This particular run was chosen to determine the effectiveness of the developed algorithms in situations where the wind noise is extremely high. Figure 2(b) shows the spectrogram of the data collected by the center microphone of node 1. As can be seen, the effects of wind noise are clearly evident in this spectrogram.

Figures 4(a)-(d) show the DOA estimation results, obtained using the arithmetic Capon, geometric Capon, harmonic Capon, and STCM algorithms, respectively. It is easily seen that the geometric and harmonic mean Capon methods provide very good DOA estimates even in presence of high level of wind noise. For this node, all the tracks are successfully detected. However, what is strange here is that both the geometric and harmonic mean Capons detect an extra track which has a trend similar to the last track (the most right hand side actual track). More interestingly, this extra track was not detected in the other nodes. At this point, we are not sure what might have caused this since the truth file for this run did not show this particular track. We note that the stationary targets cannot be detected as they are very far (approximately 4 and 8 km) from the nodes.

4.3. Observations & Conclusions

This paper presents several methods for wideband DOA estimation of multiple targets that move in closely spaced formations. It is observed that the geometric and harmonic mean wideband Capon DOA estimation algorithms provide good DOA estimates. At nominal SNR, the algorithms are able to successfully track target groups and also resolve closely spaced targets to some extent. In some scenarios where both light and heavy

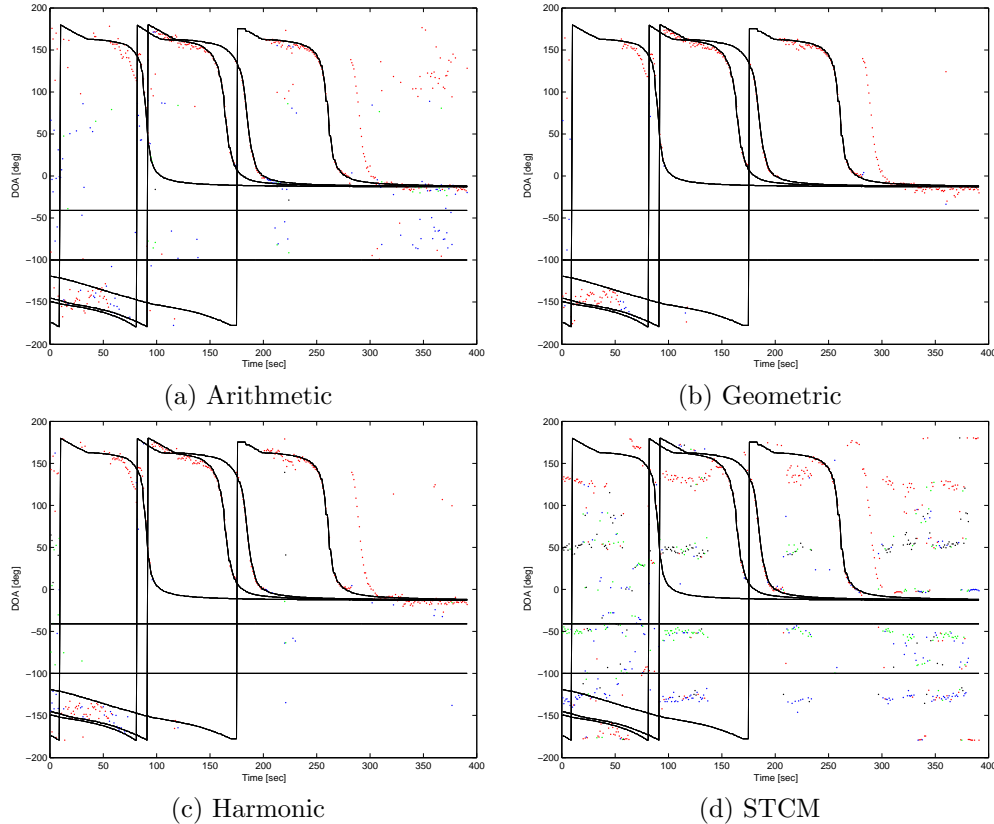


Figure 4. DOA Estimates for Run 2, obtained using Arithmetic, Geometric, Harmonic Mean Wideband Capon, and STCM Algorithms.

vehicles are present together in a run, the algorithms exhibit some difficulty tracking the light vehicles, especially at far range. By looking at the DOA estimates and also the actual range of the targets from the nodes, we can see that heavy and medium weight vehicles can be successfully detected and tracked at slightly over 1.6km (1 mile). At farther distances the detection of targets becomes more difficult. Closer investigation of the spectrogram of the first 100 seconds of node 1 of run 1 showed that for the first 40 to 50 seconds there is no indication of targets. After the 50 seconds when the group of heavy tracked vehicles are approximately 1.6km away from node 1, good DOA estimates are provided by the algorithms. It is very interesting to note that in all the cases studied the algorithms always perform better on the data collected by node 1, compared to the other two nodes. In fact, when any of the wideband Capon algorithms are used, all the target groups in node 1 are detected and tracked. For the other nodes, on the other hand, the light vehicles are usually not detected. The reason for this relatively poor performance of nodes 2 and 3 should be carefully investigated in the future.

ACKNOWLEDGMENTS

This work is funded by Army SBIR-Phase II contract # DAAE30-03-C-1055. The data and technical support has been provided by the US Army TACOM-ARDEC, Picatinny Arsenal, NJ. The authors would like to thank Bob Wade at Picatinny Arsenal for his invaluable suggestions and technical support.

REFERENCES

1. N. Srouf, "Unattended Ground Sensors- A Prospective for Operational Needs and Requirements," *ARL Report Prepared for NATO*, October 1999.

2. T. Pham and M. Fong, "Real-time implementation of MUSIC for wideband acoustic detection and tracking," *Proc. of SPIE AeroSense'97: Automatic Target Recognition VII*, Orlando, FL, April 1997.
3. T. Pham and B. M. Sadler, "Wideband Array Processing Algorithms for Acoustic Tracking of Ground Vehicles," *ARL Technical Report*, Adelphi, MD, 1997.
4. H. L. Van Trees, *Optimum Array Processing*, Wiley Interscience, 2002.
5. J. Krolik, "Focused wideband array processing for spatial spectral estimation", Chap. 6 in *Advances in Spectrum Analysis and Array Processing, Vol. II*, S. Haykin ed. Prentice-Hall, 1991.
6. H. Wang and M. Kaveh, "Coherent Signal Subspace Processing for the Detection and Estimation of Angles of Arrival of Multiple Wideband Sources", *IEEE Trans. on Acoustics, Speech and Signal Proc.*, vol. 33, pp. 823-831, 1985.
7. M. R. Azimi-Sadjadi, "Detection, Tracking and Classification of Multiple Targets using Advanced Beamforming and Classification Methods," *First-Year Summary Report, Phase II SBIR-Army*, January 2004.
8. E. D. D. Claudio, R. Parisi, "WAVES: weighted average of signal subspaces for robust wideband direction finding," *IEEE Trans. on Signal Processing*, vol.49, no.10, pp.2179-2191, 2001.
9. H. Hung and M. Kaveh, "Focusing Matrices for Coherent Signal Subspace Processing", *IEEE Trans. on Acoustics, Speech and Signal Proc.*, vol. 36, pp. 1272-1281, 1988.